Constraining the charm Yukawa and Higgs-quark coupling universality

Gilad Perez,[1,*] Yotam Soreq,[1,†] Emmanuel Stamou,[1,‡] and Kohsaku Tobioka[1,2,3,§]

[1]*Department of Particle Physics and Astrophysics, Weizmann Institute of Science, Rehovot 7610001, Israel*
[2]*Theory Center, High Energy Accelerator Research Organization (KEK), Tsukuba 305-0801, Japan*
[3]*School of Physics and Astronomy, Raymond and Beverley Sackler Faculty of Exact Sciences,*
Tel Aviv University, Tel Aviv 6997801, Israel

We introduce four different types of data-driven analyses with different levels of robustness that constrain the size of the Higgs–charm Yukawa coupling: (i) Recasting the vector-boson associated Vh analyses that search for the bottom-pair final state. We use this mode to directly and model independently constrain the Higgs-to-charm coupling, $y_c/y_c^{\mathrm{SM}} \lesssim 234$. (ii) The direct measurement of the total width, $y_c/y_c^{\mathrm{SM}} \lesssim 120$–140. (iii) The search for $h \to J/\psi\gamma$, $y_c/y_c^{\mathrm{SM}} \lesssim 220$. (iv) A global fit to the Higgs signal strengths, $y_c/y_c^{\mathrm{SM}} \lesssim 6.2$. A comparison with $t\bar{t}h$ data allows us to show that the Higgs does not couple to quarks in a universal way, as is expected in the Standard Model. Finally, we demonstrate how the experimental collaborations can further improve our direct bound by roughly an order of magnitude by charm tagging, as is already used in new-physics searches.

I. INTRODUCTION

The discovery of the Higgs boson is a triumph of the LHC [1,2] and yet another success for the Standard Model (SM) with its minimal Higgs sector of electroweak (EW) symmetry breaking (EWSB). The first run of the LHC was very successful not only because of the Higgs discovery, but also because it provided us with a rather strong qualitative test of several aspects of the Higgs mechanism: it established that the Higgs plays a dominant role in inducing the masses of the EW gauge bosons and that the Higgs coupling to the longitudinal states tames the WW scattering rates up to high energies.

However, in the minimalistic SM way of EWSB, the Higgs plays another crucial role. Namely, it induces the masses of all charged fermions. This results in a sharp prediction, free of additional input parameters, for the Higgs–fermion interaction strength

$$y_f \simeq \sqrt{2}\frac{m_f}{v}, \qquad (1)$$

where $f = u, c, t, d, s, b, e, \mu, \tau$, and $v \simeq 246$ GeV is the Higgs vacuum expectation value. This prediction holds to a very good accuracy. So far, this additional role of the Higgs has not yet been tested directly in a strong way. The best information currently available is on the Higgs couplings to the third-generation charged fermions:

*gilad.perez@weizmann.ac.il
†yotam.soreq@weizmann.ac.il
‡emmanuel.stamou@weizmann.ac.il
§kohsakut@post.tau.ac.il

$$\mu_{t\bar{t}h} = 2.4 \pm 0.8, \qquad \mu_b = 0.71 \pm 0.31,$$
$$\mu_\tau = 0.98 \pm 0.22. \qquad (2)$$

Here, we averaged the ATLAS [3–5] and CMS [6–8] results for the Higgs signal strength to fermions $\mu_f \equiv \frac{\sigma}{\sigma_{\mathrm{SM}}}\frac{\mathrm{BR}_{f\bar{f}}}{\mathrm{BR}_{f\bar{f}}^{\mathrm{SM}}}$. σ stands for the production cross section, $\mathrm{BR}_X = \mathrm{BR}(h \to X)$, and the SM script indicates the SM case. These results are consistent with the SM expectations, though the errors are still noticeably large. In contrast, our current knowledge regarding the Higgs couplings to the first two light generation fermions is significantly poorer. In fact, at this point we only have a rather weak upper bound on the corresponding signal strengths of muons and electrons [9,10],

$$\mu_\mu \le 7, \qquad \mu_e \le 4 \times 10^5, \qquad (3)$$

at a 95% confidence level (C.L.). Equations. (2) and (3) together exclude Higgs–lepton coupling universality. Direct information does not exist at present regarding the Higgs–light-quark couplings. Measuring these Higgs–light couplings is interesting for three reasons: The first, although somewhat mundane, is simply that the light-quark Yukawa couplings are parameters of the SM and as such merit a measurement. The second is that given the success of both direct and indirect tests of the SM, it is now expected that the EW gauge bosons and the top quark acquire their masses dominantly via the Higgs mechanism; this is less obvious for the first two generation quarks. The light-quark masses could be induced by other subdominant sources of EWSB—for instance, from a technicolor-like condensate. Hence,

light quarks may have suppressed or even vanishing Yukawa couplings to the Higgs. In fact, based on current knowledge, we could just add bare mass terms to the first two generation fermions and treat the SM as an effective theory that is valid up to some fairly high scale, at which "unitarity" or the weakly coupled description would break down. This is similar to the status of the EW gauge sector prior to the first run of the LHC. If we assume no coupling of light quarks to the Higgs, the unitarity bound from the $q\bar{q} \to V_L V_L$ process (where V_L is a longitudinal boson) is (see e.g. Refs. [11–13])

$$\sqrt{s} \lesssim \frac{8\pi v^2}{\sqrt{6} m_{b,c,s,d,u}}$$
$$\approx 200, 1 \times 10^3, 1 \times 10^4, 2 \times 10^5, 5 \times 10^5 \text{ TeV}. \quad (4)$$

Even stronger bounds are found when $q\bar{q} \to nV_L$ processes are considered [14]. They lead to the following corresponding unitarity constraints [15]:

$$\sqrt{s} \lesssim 23, 31, 52, 77, 84 \text{ TeV}. \quad (5)$$

These bounds are weak enough as to make the question regarding the origin of light-quark masses a fundamentally interesting question. The third argument, following a reverse reasoning, is that with new physics it is actually easy to obtain enhancements in Higgs–light-quark interaction strengths. As the Higgs is rather light, it can only decay to particles that interact very weakly with it. Within the SM, its dominant decay mode is to a bottom-quark pair. Therefore, a deformation of the Higgs couplings to the lighter SM particles, say the charm quarks (for possibly relevant discussions, see Refs. [16–25]), could compete with the Higgs–bottom coupling and would lead to a dramatic change of the Higgs phenomenology at colliders [26].

Recent theoretical and experimental progress opened a window towards studying the Higgs coupling to light quarks at future colliders. On the theoretical frontier, it was demonstrated in Ref. [26] that using inclusive charm tagging would enable the LHC experiments to search for the decay of the Higgs into a pair of charm jets (c-jets). Furthermore, it was shown that the Higgs–charm coupling may be probed by looking at exclusive decay modes involving a $c - \bar{c}$ vector meson and a photon [27]. A similar mechanism, based on exclusive decays to light-quark states and gauge bosons $\gamma/W/Z$, was shown to yield a potential access to the Higgs–light-quark couplings [28]. (See also Refs. [29–31] for studies of exclusive EW gauge boson decays.) On the experimental frontier, ATLAS has recently published two SUSY searches [32,33] that make use of charm tagging [34]. On the exclusive frontier, ATLAS searched for Higgs decays to quarkonia (e.g. J/ψ, Υ) and a

photon final state [35]. All these developments provide a proof of principle that in the future we may be able to test the Higgs mechanism of mass generation even for light quarks.

In the following, we introduce four different types of data-driven analyses with different levels of robustness that constrain the size of the Higgs-charm Yukawa coupling. This should be considered as a first step towards improving our understanding regarding the origin of light-quark masses. In the future, the methods described below are expected to yield significantly better sensitivities to the corresponding Yukawa couplings. One direct implication of our analyses is the establishment of the fact that the Higgs couples to the quarks in a nonuniversal manner.

II. SIGNAL-STRENGTH CONSTRAINT VIA $Vh(b\bar{b})$ RECAST

The ATLAS and CMS collaborations studied the Higgs decay into $b\bar{b}$ via Vh production, in which the Higgs is produced in association with a W/Z gauge boson, using 5 fb^{-1} at 7 TeV and 20 fb^{-1} at 8 TeV [4,7]. Due to the rough similarities between charm and bottom jets, jets originating from charm quarks may be mistagged as b-jets. We thus recast the existing analyses of $h \to b\bar{b}$ to study and constrain the $h \to c\bar{c}$ rate. This will provide a direct and model-independent bound on the Higgs–charm coupling. To allow the Higgs–charm coupling to float freely, the signal strength should be modified according to

$$\mu_b = \frac{\sigma \text{BR}_{b\bar{b}}}{\sigma_{\text{SM}} \text{BR}_{b\bar{b}}^{\text{SM}}}$$
$$\to \frac{\sigma \text{BR}_{b\bar{b}} \epsilon_{b_1} \epsilon_{b_2} + \sigma \text{BR}_{c\bar{c}} \epsilon_{c_1} \epsilon_{c_2}}{\sigma_{\text{SM}} \text{BR}_{b\bar{b}}^{\text{SM}} \epsilon_{b_1} \epsilon_{b_2} + \sigma_{\text{SM}} \text{BR}_{c\bar{c}}^{\text{SM}} \epsilon_{c_1} \epsilon_{c_2}}$$
$$= \left(\mu_b + \frac{\text{BR}_{c\bar{c}}^{\text{SM}}}{\text{BR}_{b\bar{b}}^{\text{SM}}} \frac{\epsilon_{c_1} \epsilon_{c_2}}{\epsilon_{b_1} \epsilon_{b_2}} \mu_c \right) \bigg/ \left(1 + \frac{\text{BR}_{c\bar{c}}^{\text{SM}}}{\text{BR}_{b\bar{b}}^{\text{SM}}} \frac{\epsilon_{c_1} \epsilon_{c_2}}{\epsilon_{b_1} \epsilon_{b_2}} \right), \quad (6)$$

where $\epsilon_{b_{1,2}}$ and $\epsilon_{c_{1,2}}$ are efficiencies to tag jets originating from bottom and charm quarks, respectively, and $\text{BR}_{c\bar{c}}^{\text{SM}}/\text{BR}_{b\bar{b}}^{\text{SM}} \simeq 5\%$ [36].

One working point for b-tagging and c-jet contamination, defined via $\epsilon_{b_{1,2}}, \epsilon_{c_{1,2}}$, constrains only one linear combination of μ_b and μ_c; it corresponds to a flat direction in the $\mu_c - \mu_b$ plane. To disentangle the flat direction, at least two tagging points with different ratios, $\epsilon_{c/b}^2 \equiv (\epsilon_{c_1} \epsilon_{c_2})/(\epsilon_{b_1} \epsilon_{b_2})$, should be adopted. ATLAS and CMS are employing different tagging working points, so combining their information allows us to constrain μ_c. The typical tagging efficiencies are given in Table I, and the combinations of working points in the analyses we use are given in Table II. In the ATLAS [4] search, there are two tagging points that have high and moderate rejection rates for c-jets, while CMS [7] has four points with relatively high acceptance of c-jets. Indeed, there are various values

TABLE I. The ATLAS and CMS b- and c-efficiencies for the different tagging criteria. The CMS working points of CSV = 0.244, 0.4, 0.5, and 0.677 are referred to as Loose, Med1, Med2, and Med3, respectively [38].

ATLAS	Med	Tight	CMS	Loose	Med1	Med2	Med3
ϵ_b	70%	50%	ϵ_b	88%	82%	78%	71%
ϵ_c	20%	3.8%	ϵ_c	47%	34%	27%	21%

TABLE II. Summary of the experimental results used for the recast of the $Vh(b\bar{b})$ searches. Figures are taken from Refs. [4] and [7] for ATLAS and CMS, respectively.

	Figures	1st tag	2nd tag	$\epsilon_{c/b}^2$
(a) ATLAS	11, 12(a,b,d), 13, 17	Med	Med	0.082
(b) ATLAS	12(c)	Tight	Tight	0.059
(c) CMS	10,11,12	Med1	Med1	0.18
(d) CMS	13 Left	Med2	Loose	0.19
(e) CMS	13 Right	Med1	Loose	0.23
(f) CMS	14	Med3	Loose	0.16

of $\epsilon_{c/b}^2$, categories (a)–(f) in Table II. The tagging efficiencies do have a p_T^{jet} dependence, but we have verified that the ratio of efficiencies, such as $\epsilon_{c/b}^2$, is less sensitive to the p_T^{jet}; see Refs. [37,38]. Hereafter, we assume the efficiencies for each analysis to be constant.

For our recast study, we proceed as follows: From existing data, summarized in Table II, we use all the bins of the boosted decision tree output with $S/B \geq 0.025$; those with lower ratios are simply background dominated. We then adopt the modified signal strength according to Eq. (6) with $\epsilon_{c/b}^2$ depending on the category. We have constructed a likelihood function, $L(\mu_c, \mu_b)$, that is evaluated by a Poisson probability distribution convoluted with the Monte Carlo systematic error with Gaussian weights. For a parameter estimate, we use the likelihood ratio,

$$\lambda(\mu_c, \mu_b) = -2 \log \frac{L(\mu_c, \mu_b)}{L(\hat{\mu}_c, \hat{\mu}_b)}, \qquad (7)$$

where $\hat{\mu}_c$ and $\hat{\mu}_b$ are values at the best-fit point. In Fig. 1, we show the 68.3% C.L. and 95% C.L. contours, as well as 68.3% C.L. bands corresponding to each analysis (a)–(f). As discussed above, while the constraint of a given analysis is a flat direction in the $\mu_c - \mu_b$ plane, the combination of different analyses disentangles the degeneracy, leading to an ellipse. We further obtain the bound on μ_c with profiled μ_b (method of profile likelihood ratio [39]):

$$\mu_c = 95^{+90(175)}_{-95(180)} \quad \text{at } 68.3(95)\% \text{ C.L.} \qquad (8)$$

This is the first direct and model-independent bound on the charm signal strength.
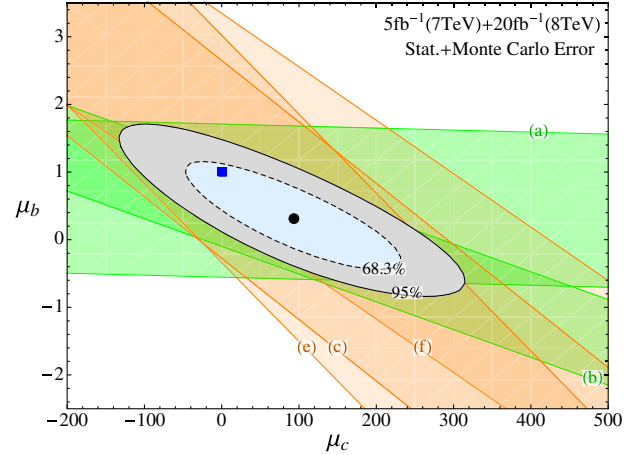

FIG. 1 (color online). 68.3% C.L. (cyan) and 95% C.L. (gray) allowed regions in the $\mu_c - \mu_b$ plane. The best-fit (SM) point is indicated by the black circle (blue rectangle). The green (orange) bands are the 68.3% C.L. bands obtained from ATLAS (CMS) data. The labels (a)–(f) refer to the criteria in Table II. Note that region (d) is not shown because it is too broad.

III. NEW PRODUCTION OF Vh AND CHARM YUKAWA

We would like to interpret the constraint of Eq. (8) as an upper bound on the charm Yukawa or, equivalently, on $\kappa_c \equiv y_c/y_c^{SM}$. Similar κ definitions hold for all Higgs couplings. Relative signs between κ's do not affect our main results, and we thus stick to $\kappa_X > 0$.

Assuming no modification of the production with respect to the SM restricts the Higgs-to-charm signal strength to be

$$\mu_c = BR_{c\bar{c}}/BR_{c\bar{c}}^{SM} \lesssim 34. \qquad (9)$$

The bound in Eq. (8) is weaker than the one in Eq. (9). Thus, it cannot bound κ_c from above; namely, the inequality is satisfied even in the $\kappa_c \to \infty$ or $BR_{c\bar{c}} \to 1$ limit.

However, as κ_c (or more generally $\kappa_{u,d,s,c}$) becomes large, new contributions to the same final states, shown in Fig. 2, become important and eliminate the "runaway" to arbitrarily large Yukawa. The contributions to the Vh production cross section as a function of κ_c are presented in Fig. 3 and roughly given by

$$\frac{\sigma_{pp \to Vh}}{\sigma_{pp \to Vh}^{SM}} \simeq 1 + \left(\frac{\kappa_c}{\lambda_c}\right)^2 \quad \text{with} \quad \lambda_c = 75\text{–}200 \qquad (10)$$
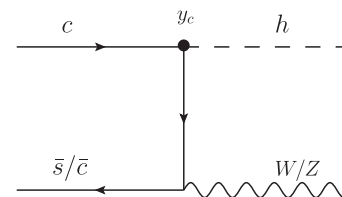

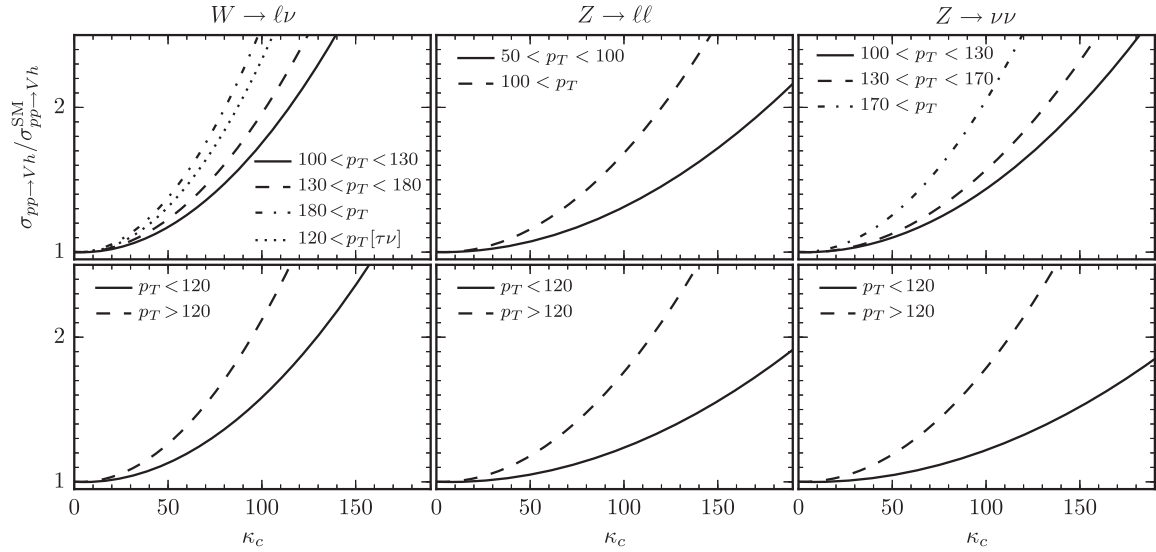FIG. 2. Example diagram that modifies Vh production when the charm-quark Yukawa is enhanced.

FIG. 3. Vh enhancement with κ_c from the new production mechanism, using the preselection cuts of CMS and ATLAS.

for large κ_c, where the exact value of λ_c depends on the channel. Here, the Higgs coupling to the W/Z is assumed to be SM-like, i.e. $\kappa_V = 1$. We obtained these results using MadGraph 5.2 [40] at the parton level and at leading order applying the CMS [7] and ATLAS [4] selection cuts for the LHC 8 TeV run. For a more complete treatment of the new production mechanisms, including the contributions from u, d, s, and also those to final states with VBF-like topology, and comparison with future machines, we refer the reader to the companion paper [41].

The new production mechanism significantly enhances the production cross section for large Yukawa, which is disfavored by the Vh data. In Fig. 4, we thus combine
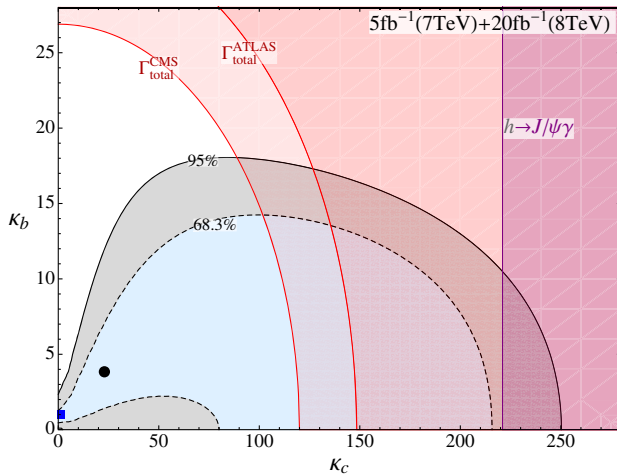

FIG. 4 (color online). 68.3% C.L. (cyan) and 95% C.L. (gray) allowed regions of the recast study in the $\kappa_c - \kappa_b$ plane, with the best-fit (SM) point indicated by the black circle (blue rectangle). Shaded areas represent the regions excluded by the total width (ATLAS and CMS) and the exclusive Higgs decay of $h \to J/\psi\gamma$.

ATLAS and CMS data to constrain both κ_c and κ_b. The allowed 68.3% (95%) C.L. region is in blue (gray). The mapping between the signal strength and the Yukawa couplings, i.e. Figs. 1 and 4, can be qualitatively understood by the relations

$$\mu_{c/b} \approx \left(1 + \frac{\kappa_c^2}{\lambda_c^2}\right) \frac{\kappa_{c/b}^2}{1 + (\kappa_b^2 - 1)\mathrm{BR}_{b\bar{b}}^{\mathrm{SM}} + (\kappa_c^2 - 1)\mathrm{BR}_{c\bar{c}}^{\mathrm{SM}}}. \tag{11}$$

From this also the mapping of the best-fit points in the two plots can be understood. Profiling over κ_b yields an upper bound on the charm Yukawa:

$$\kappa_c \lesssim 234 \quad \text{at 95\% C.L.} \tag{12}$$

IV. THE TOTAL WIDTH

Both ATLAS and CMS give a model-independent bound on the Higgs total width from the invariant-mass distribution of the $h \to 4\ell$ and $h \to \gamma\gamma$ signals. These bounds are limited by the experimental resolution of approximately 1 GeV. Assuming no interference with the background, the upper limits by ATLAS [42] and CMS [43] are

$$\Gamma_{\text{total}} < \begin{cases} 2.4, 5.0 \text{ GeV (CMS, ATLAS)} & h \to \gamma\gamma \\ 3.4, 2.6 \text{ GeV (CMS, ATLAS)} & h \to 4\ell \\ 1.7 \text{ GeV (CMS) combined} & h \to \gamma\gamma, 4\ell \end{cases}$$

$$\tag{13}$$

at 95% C.L. This should be compared with the SM prediction of $\Gamma_{\text{total}}^{\mathrm{SM}} = 4.07$ MeV [36] for $m_h = 125$ GeV. We use the above upper bound on the total width to bound

the charm Yukawa by assuming that the entire Higgs width is saturated by it:

$$\kappa_c^2 \mathrm{BR}_{c\bar{c}}^{\mathrm{SM}} \Gamma_{\mathrm{total}}^{\mathrm{SM}} = 1.18 \times 10^{-4} \kappa_c^2 \ \mathrm{GeV} < \Gamma_{\mathrm{total}}, \qquad (14)$$

with $\mathrm{BR}_{c\bar{c}}^{\mathrm{SM}} = 2.9 \times 10^{-2}$. The corresponding upper bounds at 95% C.L. from Eq. (13) are

$$\kappa_c < 120 (\mathrm{CMS}), \qquad \kappa_c < 150 (\mathrm{ATLAS}), \qquad (15)$$

where in the case of ATLAS we have used the bound from $h \to 4\ell$, and in the case of CMS the combined bound.

V. INTERPRETATION OF $h \to J/\psi\gamma$

Very recently, ATLAS set the first bound on the exclusive Higgs decay to $J/\psi\gamma$ [35]:

$$\sigma \mathrm{BR}_{J/\psi\gamma} < 33 \ \mathrm{fb} \quad \text{at 95\% C.L.} \qquad (16)$$

Under the assumption of SM Higgs production, this can be interpreted as a bound of $\mathrm{BR}(h \to J/\psi\gamma) < 1.5 \times 10^{-3}$. The partial width of $h \to J/\psi\gamma$ is given by [44]

$$\Gamma_{J/\psi\gamma} = 1.42 [(1.0 \pm 0.017)\kappa_\gamma - (0.087 \pm 0.012)\kappa_c]^2 \\ \times 10^{-8} \ \mathrm{GeV}. \qquad (17)$$

The dependence on the production mechanism and the Higgs total width can be canceled to a good approximation in the ratio between the bound (or measurement in the future) of the $h \to J/\psi\gamma$ rate and one of the other Higgs rate measurements with inclusive production, for example $h \to ZZ^* \to 4\ell$. We define

$$\mathcal{R}_{J/\psi, Z} = \frac{\sigma \mathrm{BR}_{J/\psi\gamma}}{\sigma \mathrm{BR}_{ZZ^* \to 4\ell}} \simeq \frac{\Gamma_{J/\psi\gamma}}{\Gamma_{ZZ^* \to 4\ell}} \\ = 2.79 \frac{(\kappa_\gamma - 0.087\kappa_c)^2}{\kappa_V^2} \times 10^{-2}, \qquad (18)$$

where a perfect cancellation of the production is assumed (correct to leading order) and $\mathrm{BR}_{ZZ^* \to 4\ell}^{\mathrm{SM}} = 1.26 \times 10^{-4}$ [36]. Using Eq. (16) and the ZZ^* signal strength $\mu_{ZZ^*} = 1.44^{+0.40}_{-0.33}$ [45], we extract

$$\mathcal{R}_{J/\psi, Z} = \frac{\sigma \mathrm{BR}_{J/\psi\gamma}}{\mu_{ZZ^*} \sigma_{\mathrm{SM}} \mathrm{BR}_{ZZ^* \to 4\ell}^{\mathrm{SM}}} < 9.3 \qquad (19)$$

at 95% C.L. Combining the last two equations leads to

$$-210\kappa_V + 11\kappa_\gamma < \kappa_c < 210\kappa_V + 11\kappa_\gamma. \qquad (20)$$

This yields the bound $\kappa_c \lesssim 220$, assuming that κ_γ and κ_V (see discussion below) and also the Higgs decay width to a Z and two leptons (e.g. $h \to Z\gamma^* \to 4\ell$) are all close to their respective SM values.

VI. GLOBAL ANALYSIS

A global analysis of the Higgs data leads to an indirect bound on the Higgs total width and untagged decay width, see e.g. Refs. [46–53]. In the absence of non-SM production mechanisms, the allowed range for untagged decays is the leading bound on the charm Yukawa. For this, we can safely ignore non-SM Vh and VBF-like production enhancements because they are found to be negligible for $\kappa_c \lesssim 50$. The allowed range of κ_V from EW precision data assuming a cutoff scale of 3 TeV is $\kappa_V = 1.08 \pm 0.07$ [50]. This, along with the Higgs measurement of VBF and gluon fusion in WW^*, ZZ^*, and $\tau\bar{\tau}$ final states, results in a much stronger bound on the total Higgs width than the direct measurement.

Following the analysis of Ref. [26], we consider the current available Higgs data from ATLAS [3–5,45,54–57], CMS [6–8,10,43,58–61] and Tevatron [62,63], extracted by using Ref. [64], along with the EW data as in Ref. [50]. We find that the 95% C.L. allowed range for the charm Yukawa is

$$\kappa_c \lesssim 6.2, \qquad (21)$$

where all the Higgs couplings (including $h \to WW, ZZ$, $\gamma\gamma, gg, Z\gamma, b\bar{b}, \tau\bar{\tau}$) were allowed to vary from their SM values. Allowing the up-quark Yukawa also to vary does not change this bound. Note that the bound in Eq. (21) depends on the global fit assumption, in particular the LEP constraints, and as such carries model dependence.

The ratio between the on-shell and the off-shell $h \to ZZ^{(*)}$ rates can probe the Higgs width [65]. The current bounds are at the order of $\Gamma_{\mathrm{total}}/\Gamma_{\mathrm{total}}^{\mathrm{SM}} \lesssim 5.4, 7.7$ from CMS [66] and ATLAS [67], respectively. This corresponds to $\kappa_c \lesssim 14, 16$. However, as pointed out in Ref. [68], these bounds are model dependent. Thus, we do not further consider this bound in our analysis. We mention that low-energy processes can also indirectly constrain light-quark Yukawas; see for example Refs. [69–71].

VII. HIGGS-QUARK NONUNIVERSALITY

We now turn to provide a lower bound on the top Yukawa coupling in order to compare it with the upper bounds on the charm Yukawa coupling obtained above. A comparison with $t\bar{t}h$ data allows us to show that current data eliminate the possibility that the Higgs couples to quarks in a universal way, as is expected in the SM. As mentioned in Eq. (2), a naive average of the ATLAS and CMS results yields $\mu_{t\bar{t}h} = 2.4 \pm 0.8$. This leads to a lower bound on the top Yukawa (at 95% C.L.),

$$\kappa_t > 0.9 \sqrt{\frac{\mathrm{BR}_{\mathrm{finals}}^{\mathrm{SM}}}{\mathrm{BR}_{\mathrm{finals}}}} > 0.9, \qquad (22)$$

where BR$_{finals}$ stands for the final states that were considered by the collaborations in the $t\bar{t}h$ measurements. The last inequality is valid in the case in which the Higgs-to-charm pairs is the dominant partial width (as is expected in the case where our rather weak bounds obtained above are saturated). In the special case where the dominant decays are to charms and τ's, namely $\kappa_\tau \gg 1$, we have $\mu_{VBF,\tau} > 2$, which is excluded by data [5,8]. We thus conclude that

$$\frac{y_c}{y_t} = \frac{\kappa_c}{\kappa_t}\frac{y_c^{SM}}{y_t^{SM}} \simeq \frac{1}{280} \times \frac{\kappa_c}{\kappa_t} \Rightarrow y_c < y_t, \qquad (23)$$

where the last inequality is based on a comparison of Eqs. (12), (15), (20) and (21) with Eq. (22). We therefore conclude that the Yukawa couplings of the up-type quarks are nonuniversal.

VIII. SUMMARY OF LHC CONSTRAINTS

In Fig. 4, we present bounds on Higgs couplings from the Vh recast, the total width measurements, and the exclusive decay to $J/\psi\gamma$ on the $\kappa_c - \kappa_b$ plane. We see that the relatively robust bounds from the Vh recast and the total width measurements are of the same order of magnitude and also complement each other.

In Fig. 5, we show the 95% C.L. regions for the Higgs couplings to fermions as a function of their masses based on the global analysis, and we have added the bounds obtained above regarding the charm Yukawa coupling.

An improvement of the bound on the charm signal strength can be achieved by adopting the charm tagging [34]. We estimate the sensitivity from current data as follows: We rescale the expected number of signal and background events of the 8 TeV ATLAS analysis (Table 8 of Ref. [4]) according to the efficiencies of the charm tagging [33],
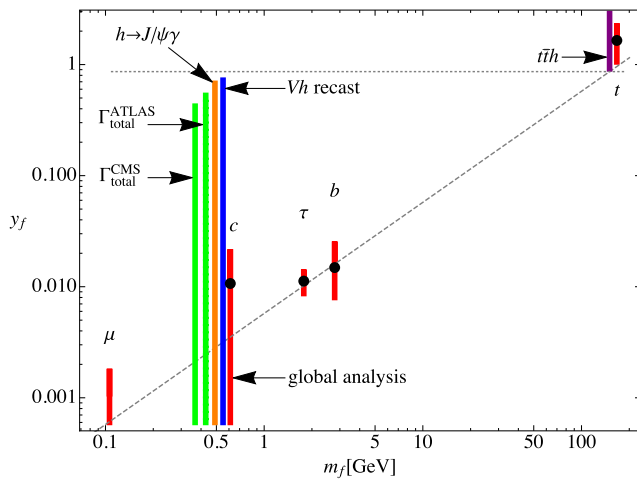
$$\epsilon_b = 13\%, \qquad \epsilon_c = 19\%, \qquad \epsilon_l = 0.5\%, \quad (24)$$

where ϵ_l is efficiency to tag light jets. Here, we assume that medium b-tagging in Table I ($\epsilon_l = 1.25\%$) is used in the analysis and that the decomposition of the $W(Z)+$ heavy-flavor quarks background is 35% (20%) $W(Z)+$ $c\bar{c}$ and 65% (80%) $W(Z) + b\bar{b}$. We combine the rescaled ATLAS analysis with the CMS results (c)–(f) in Table II and obtain an uncertainty of

$$\Delta\mu_c \simeq 50(107) \qquad (25)$$

at a 68.3% (95%) C.L. We see that even with the same luminosity, the error is significantly reduced with respect to the one in Eq. (8).

IX. FUTURE LHC PROSPECTS

Finally, we estimate the future sensitivity at the LHC. We utilize results of Tables 6–9 in Ref. [72], where ATLAS performed a dedicated Monte Carlo study of $Vh(b\bar{b})$ in the one- and two-lepton final states for LHC run II with 300 fb^{-1} and the LHC high-luminosity upgrade (HL-LHC) with 3000 fb^{-1} at 14 TeV. From the given working point of medium b-tagging, we rescale the signal and background of the one-lepton final state to those in charm tagging. We leave the two-lepton analysis as original because, as discussed, we need at least two working points to extract μ_b and μ_c independently. We then also assume that the same analysis can be performed by CMS.

The future sensitivity reach for μ_c is shown as ellipses in the $\mu_c - \mu_b$ plane in Fig. 6. Here, we take into account only the statistical error. The expected uncertainty with profiled μ_b reads
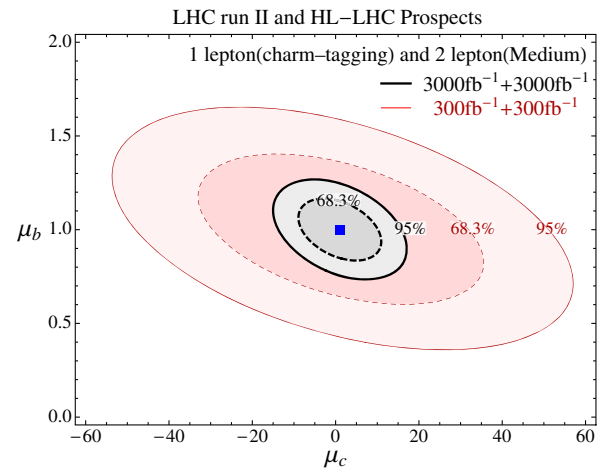

FIG. 5 (color online).   Summary of current constraints on the Higgs couplings to fermions, including the new bounds on the charm Yukawa.

FIG. 6 (color online).   Expected reach for the signal-strength measurement of $h \to b\bar{b}$ and $h \to c\bar{c}$ at the LHC run II and HL-LHC: The thick black (thin purple) curves correspond to the reach with 3000 (300) fb^{-1}. The solid (dashed) ones correspond to the 68.3% (95%) C.L. The SM expectation is $\mu_{b,c} = 1$.

$$\Delta\mu_c = \begin{cases} 23(45) & \text{with} \quad 2\times300 \text{ fb}^{-1} \\ 6.5(13) & \text{with} \quad 2\times3000 \text{ fb}^{-1} \end{cases} \quad (26)$$

at a 68.3% (95%) C.L. Compared to the result of LHC run I, the uncertainty is improved by roughly an order of magnitude with 3000 fb^{-1} thanks to charm tagging. In the future, one may hope that the charm-tagging performance will be further optimized. As an example for such a case, we have considered the following improved charm-tagging point: $\epsilon_b = 20\%$, $\epsilon_c = 40\%$ and $\epsilon_l = 1.25\%$. As a consequence, the bounds will be further strengthened: $\Delta\mu_c \simeq 20(6.5)$ at 95% C.L. with an integrated luminosity of $2\times300(2\times3000)$ fb^{-1}.

X. CONCLUSIONS

We have performed four different analyses to constrain the charm Yukawa and obtained the following bounds:

$$\frac{y_c}{y_c^{SM}} \lesssim 234, 120(140), 220, 6.2, \quad (27)$$

which correspond to a recast of the $h \to b\bar{b}$ searches, the direct bound on the Higgs total width at CMS (ATLAS), the exclusive decay of $h \to J/\psi\gamma$, and the global analysis, respectively. Together with the $t\bar{t}h$ analyses of ATLAS and CMS, we conclude that the Higgs coupling to the top and charm quarks is not universal. We further point out two new production mechanisms, related to Vh and VBF processes that become important when the first two generation quarks have enhanced couplings to the Higgs. In conjunction with a future measurement at an electron-positron collider (linear or circular), the former mechanism is sensitive to the Higgs–light-quark couplings. We also provide projections for the sensitivity of the LHC experiments to the charm Yukawa by adopting a dedicated charm-tagging analysis resulting in an order of magnitude improvement. Finally, we point out that with the recent installation of the Insertable B-Layer (IBL) subdetector [73], the ATLAS capability for charm tagging is expected to be further improved, enhancing the sensitivity to the Higgs–charm coupling.

[1] G. Aad *et al.* (ATLAS Collaboration), Phys. Lett. B **716**, 1 (2012).

[2] S. Chatrchyan *et al.* (CMS Collaboration), Phys. Lett. B **716**, 30 (2012).

[3] ATLAS Collaboration, Reports No. ATLAS-CONF-2014-011, No. ATLAS-COM-CONF-2014-004, 2014.

[4] G. Aad *et al.* (ATLAS Collaboration), J. High Energy Phys. 01 (2015) 069.

[5] G. Aad *et al.* (ATLAS Collaboration), J. High Energy Phys. 04 (2015) 117.

[6] V. Khachatryan *et al.* (CMS Collaboration), J. High Energy Phys. 09 (2014) 087.

[7] S. Chatrchyan *et al.* (CMS Collaboration), Phys. Rev. D **89**, 012003 (2014).

[8] S. Chatrchyan *et al.* (CMS Collaboration), J. High Energy Phys. 05 (2014) 104.

[9] G. Aad *et al.* (ATLAS Collaboration), Phys. Lett. B **738**, 68 (2014).

[10] V. Khachatryan *et al.* (CMS Collaboration), Phys. Lett. B **744**, 184 (2015).

[11] R. S. Chivukula, N. D. Christensen, B. Coleppa, and E. H. Simmons, Phys. Rev. D **75**, 073018 (2007).

[12] W. J. Marciano, G. Valencia, and S. Willenbrock, Phys. Rev. D **40**, 1725 (1989).

[13] T. Appelquist and M. S. Chanowitz, Phys. Rev. Lett. **59**, 2405 (1987).

[14] F. Maltoni, J. M. Niczyporuk, and S. Willenbrock, Phys. Rev. Lett. **86**, 212 (2001).

[15] D. A. Dicus and H.-J. He, Phys. Rev. D **71**, 093009 (2005).

[16] C. Delaunay, C. Grojean, and G. Perez, J. High Energy Phys. 09 (2013) 090.

[17] C. Delaunay, T. Flacke, J. Gonzalez-Fraile, S. J. Lee, G. Panico, and G. Perez, J. High Energy Phys. 02 (2014) 055.

[18] M. Blanke, G. F. Giudice, P. Paradisi, G. Perez, and J. Zupan, J. High Energy Phys. 06 (2013) 022.

[19] R. Mahbubani, M. Papucci, G. Perez, J. T. Ruderman, and A. Weiler, Phys. Rev. Lett. **110**, 151804 (2013).

[20] A. L. Kagan, G. Perez, T. Volansky, and J. Zupan, Phys. Rev. D **80**, 076002 (2009).

[21] A. Dery, A. Efrati, G. Hiller, Y. Hochberg, and Y. Nir, J. High Energy Phys. 08 (2013) 006.

[22] G. F. Giudice and O. Lebedev, Phys. Lett. B **665**, 79 (2008).

[23] L. Da Rold, C. Delaunay, C. Grojean, and G. Perez, J. High Energy Phys. 02 (2013) 149.

[24] K.-F. Chen, W.-S. Hou, C. Kao, and M. Kohda, Phys. Lett. B **725**, 378 (2013).

[25] A. Dery, A. Efrati, Y. Nir, Y. Soreq, and V. Susič, Phys. Rev. D **90**, 115022 (2014).

[26] C. Delaunay, T. Golling, G. Perez, and Y. Soreq, Phys. Rev. D **89**, 033014 (2014).

[27] G. T. Bodwin, F. Petriello, S. Stoynev, and M. Velasco, Phys. Rev. D **88**, 053003 (2013).

[28] A. L. Kagan, G. Perez, F. Petriello, Y. Soreq, S. Stoynev, and J. Zupan, Phys. Rev. Lett. **114**, 101802 (2015).

[29] M. Mangano and T. Melia, Eur. Phys. J. C **75**, 258 (2015).

[30] T.-C. Huang and F. Petriello, Phys. Rev. D **92**, 014007 (2015).

[31] Y. Grossman, M. König, and M. Neubert, J. High Energy Phys. 04 (2015) 101.

[32] G. Aad *et al.* (ATLAS Collaboration), Phys. Rev. D **90**, 052008 (2014).

[33] G. Aad *et al.* (ATLAS Collaboration), Phys. Rev. Lett. **114**, 161801 (2015).

[34] CERN, Technical Report No. ATL-PHYS-PUB-2015-001, 2015.

[35] G. Aad *et al.* (ATLAS Collaboration), Phys. Rev. Lett. **114**, 121801 (2015).

[36] S. Heinemeyer *et al.* (LHC Higgs Cross Section Working Group), Report No. 10.5170/CERN-2013-004.

[37] ATLAS Collaboration, Reports No. ATLAS-CONF-2014-046, No. ATLAS-COM-CONF-2013-087.

[38] S. Chatrchyan *et al.* (CMS Collaboration), J. Instrum. **8**, P04013 (2013).

[39] G. Cowan, K. Cranmer, E. Gross, and O. Vitells, Eur. Phys. J. C **71**, 1554 (2011).

[40] J. Alwall, M. Herquet, F. Maltoni, O. Mattelaer, and T. Stelzer, J. High Energy Phys. 06 (2011) 128.

[41] G. Perez, Y. Soreq, E. Stamou, and K. Tobioka (to be published).

[42] G. Aad *et al.* (ATLAS Collaboration), Phys. Rev. D **90**, 052004 (2014).

[43] V. Khachatryan *et al.* (CMS Collaboration), Eur. Phys. J. C **75**, 212 (2015).

[44] G. T. Bodwin, H. S. Chung, J.-H. Ee, J. Lee, and F. Petriello, Phys. Rev. D **90**, 113010 (2014).

[45] G. Aad *et al.* (ATLAS Collaboration), Phys. Rev. D **91**, 012006 (2015).

[46] D. Carmi, A. Falkowski, E. Kuflik, T. Volansky, and J. Zupan, J. High Energy Phys. 10 (2012) 196.

[47] P. P. Giardino, K. Kannike, M. Raidal, and A. Strumia, Phys. Lett. B **718**, 469 (2012).

[48] J. Espinosa, C. Grojean, M. Muhlleitner, and M. Trott, J. High Energy Phys. 12 (2012) 045.

[49] J. Ellis and T. You, J. High Energy Phys. 09 (2012) 123.

[50] A. Falkowski, F. Riva, and A. Urbano, J. High Energy Phys. 11 (2013) 111.

[51] J. R. Espinosa, M. Muhlleitner, C. Grojean, and M. Trott, J. High Energy Phys. 09 (2012) 126.

[52] B. A. Dobrescu and J. D. Lykken, J. High Energy Phys. 02 (2013) 073.

[53] P. Bechtle, S. Heinemeyer, O. Stål, T. Stefaniak, and G. Weiglein, J. High Energy Phys. 11 (2014) 039.

[54] G. Aad *et al.* (ATLAS Collaboration), Phys. Rev. D **90**, 112015 (2014).

[55] ATLAS Collaboration, Reports No. ATLAS-CONF-2013-075, No. ATLAS-COM-CONF-2013-069, 2013.

[56] ATLAS Collaboration, Reports No. ATLAS-CONF-2014-060, No. ATLAS-COM-CONF-2014-078, 2014.

[57] ATLAS Collaboration, Reports No. ATLAS-CONF-2014-061, No. ATLAS-COM-CONF-2014-080, 2014.

[58] S. Chatrchyan *et al.* (CMS Collaboration), J. High Energy Phys. 01 (2014) 096.

[59] S. Chatrchyan *et al.* (CMS Collaboration), Phys. Rev. D **89**, 092007 (2014).

[60] V. Khachatryan *et al.* (CMS Collaboration), Eur. Phys. J. C **74**, 3076 (2014).

[61] CMS Collaboration, Report No. CMS-PAS-HIG-13-017, 2013.

[62] T. Aaltonen *et al.* (CDF Collaboration), Phys. Rev. D **88**, 052013 (2013).

[63] V. M. Abazov *et al.* (D0 Collaboration), Phys. Rev. D **88**, 052011 (2013).

[64] P. Bechtle, S. Heinemeyer, O. Stål, T. Stefaniak, and G. Weiglein, Eur. Phys. J. C **74**, 2711 (2014).

[65] F. Caola and K. Melnikov, Phys. Rev. D **88**, 054024 (2013).

[66] V. Khachatryan *et al.* (CMS Collaboration), Phys. Lett. B **736**, 64 (2014).

[67] ATLAS Collaboration, Reports No. ATLAS-CONF-2014-042, No. ATLAS-COM-CONF-2014-052, 2014.

[68] C. Englert and M. Spannowsky, Phys. Rev. D **90**, 053003 (2014).

[69] G. Isidori, A. V. Manohar, and M. Trott, Phys. Lett. B **728**, 131 (2014).

[70] R. Harnik, J. Kopp, and J. Zupan, J. High Energy Phys. 03 (2013) 026.

[71] F. Goertz, Phys. Rev. Lett. **113**, 261803 (2014).

[72] ATLAS Collaboration, Report No. ATL-PHYS-PUB-2014-011, 2014.

[73] M. Capeans, G. Darbo, K. Einsweiller, M. Elsing, T. Flick, M. Garcia-Sciveres, C. Gemme, H. Pernegger, O. Rohne, and R. Vuillermet, Technical Reports No. CERN-LHCC-2010-013, No. ATLAS-TDR-19, 2010.